Forcing of the Austral Autumn Surface Pressure Change over the Antarctic Continent*

THOMAS R. PARISH AND YUHANG WANG+

Department of Atmospheric Science, University of Wyoming, Laramie, Wyoming

DAVID H. BROMWICH

Polar Meteorology Group, Byrd Polar Research Center, Ohio State University, Columbus, Ohio

(Manuscript received 12 May 1995, in final form 21 June 1996)

ABSTRACT

Pronounced seasonal variations in the surface pressure field are present over the Antarctic continent. Surface pressures over the ice sheet decrease during the austral autumn period January–April and increase during the austral springtime months September–December. The largest changes are found over the highest portions of the Antarctic ice sheets where seasonal surface pressure changes of up to 20 hPa are common. The outstanding feature of these surface pressure changes is that typically the isallobaric contours closely follow the Antarctic orography during both transition periods, suggesting a strong seasonal diabatic adjustment within the lower troposphere. During austral autumn, the pronounced cooling of the lower atmosphere adjacent to the ice sheets leads to an enhancement of the Antarctic katabatic wind regime and hence the lower branch of the mean meridional circulation over the high southern latitudes. The mass transport provided by these drainage flows is proposed as the mechanism behind the autumn pressure falls. Numerical simulations of the evolution of the Antarctic katabatic wind regime indicate that the radiative cooling of the sloping ice fields and attendant mass transport result in a modification of the temperature and pressure fields in the lower troposphere similar to what is seen during the early austral autumn period.

1. Introduction

The time-averaged annual march of surface pressure over Antarctica displays large seasonal variations. Such changes in surface pressure are especially pronounced during the austral autumn and springtime transition periods when the ice sheets are subjected to rapid and dramatic changes in the intensity of solar radiation. It has been observed that surface pressures over Antarctica rise by up to 20 hPa during austral springtime from September to December and decrease by a somewhat smaller amount during the austral autumn months January to April. An example of the seasonal surface pressure change is illustrated in Fig. 1, which shows the multiannual surface pressure deviations about the annual mean for three stations situated on the high Antarctic plateau. The traces for South Pole, Vostok (78.5°S, 107°E), and Dome C (74.5°S, 123°E) display nearly identical autumn surface pressure falls of roughly 14 hPa and springtime surface pressure rises of approximately 22 hPa.

The seasonal cycle of surface pressure in the high southern latitudes has been addressed by a number of authors. Much of the literature has focused on the semiannual periodicity in surface pressure observed in the middle to polar latitudes. Schwerdtfeger and Prohaska (1956), Schwerdtfeger (1960, 1967), van Loon (1967, 1972) and van Loon and Rogers (1984), among others, have noted that a pronounced semiannual oscillation (SAO) in the surface pressure is present in the middle to high southern latitudes. The maxima in surface pressure at southern latitudes poleward of approximately 65°S occurs at the solstices and at middle latitudes near the equinoxes. The annual course of surface pressure implies a mass flow towards Antarctica from September to January and again from April to June, with mass transports equatorward from January to April and again from June to September. It was initially proposed that the SAO was a result of the different solar heating of different latitude belts (Schwerdtfeger and Prohaska 1956). In addition, van Loon (1967) has noted that the heat budget of the oceanic upper layers significantly influences the rates of heating and cooling of the different latitude belts. More recently, Meehl (1991) has reexamined the SAO using an expanded observational

* Byrd Polar Research Center Contribution Number 1044.
+ Current affiliation: Department of Earth and Planetary Sciences, Harvard University, Cambridge, Massachusetts.

Corresponding author address: Dr. Thomas R. Parish, Dept. of Atmospheric Sciences, University of Wyoming, P.O. Box 3038, Laramie, WY 82071-3038.
E-mail: parish@grizzly.uwyo.edu

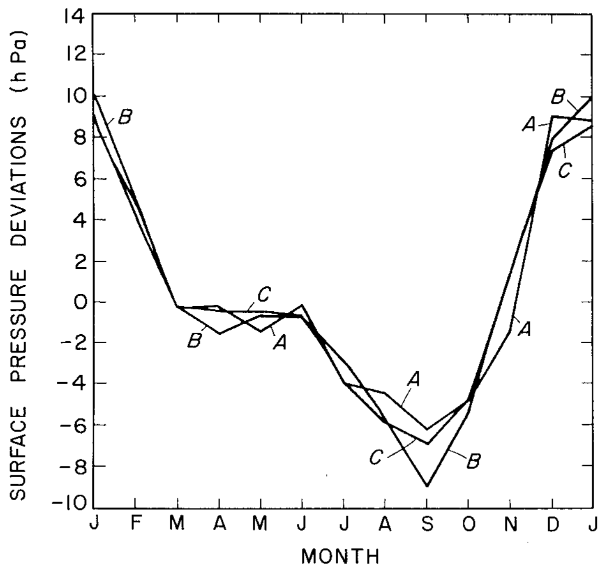

FIG. 1. Mean monthly surface pressure deviations from the mean surface pressure for Dome C (curve *A*, mean pressure 644.9 hPa), Vostok (*B*, 624.8 hPa), and South Pole (*C*, 681.3 hPa).

dataset and GCM simulations and has confirmed van Loon's hypotheses regarding the importance of the different annual cycles of temperature between Antarctica and the surrounding southern oceans in producing the SAO.

2. Discussion

Surface pressure changes during both the austral autumn and springtime transitional periods appear to be maximized over the high interior of Antarctica and decrease rapidly northward from the continental coastline such that the phase of the mass loading cycle becomes reversed between 50° and 60°S (see Schwerdtfeger 1984, Fig. 6.8). Data collected by automatic weather stations situated atop the Antarctic interior (e.g., Keller et al. 1994) evoke a similar interpretation. The seasonal changes have previously been shown to be well represented in general circulation models (Parish et al. 1994). As an example, Fig. 2 illustrates the mean monthly surface pressure differences from January to April (Fig. 2a) and again from September to December (Fig. 2b) for a 5-yr seasonal cycle experiment with the National Center for Atmospheric Research Community Climate Model Version 1 (CCM1; see also Tzeng et al. 1993). Note that the isallobaric pattern is centered over the high plateau of Antarctica. Such patterns are not an artifact of the CCM1. Operational model analyses show similar trends in the seasonal movement of mass in the high southern latitudes as well. Figure 3 illustrates the mean monthly changes in surface pressure from January to April 1987 (Fig. 3a) and from September to December 1990 (Fig. 3b) based on the European Centre for Medium-Range Weather Forecasts (ECMWF) analyses. Although significant year-to-year fluctuations occur, ECMWF analyses for other years often display mean monthly surface pressure change patterns during the transition periods similar to those shown in Fig. 3. The examples shown are best illustrative of the seasonal changes. The outstanding feature in both Figs. 2 and 3 is the close association between the contours of seasonal surface pressure changes over the Antarctic and the height contours of the underlying continental ice sheet. Comparison of the isallobaric patterns over Antarctica in Figs. 2 and 3 with the model topographies as represented in CCM1 and ECMWF (Fig. 4) reveals a striking coherence. The isallobars in both Figs. 2 and 3 ap-

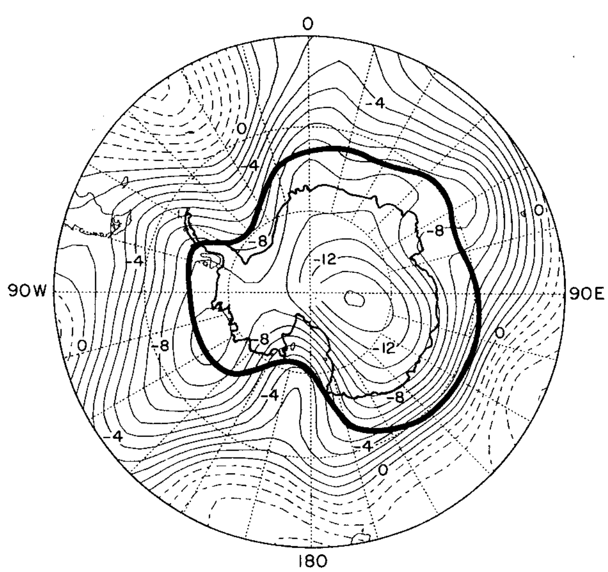

FIG. 2. Five-year average mean monthly surface pressure differences from (a) January–April and (b) September–December for 5-yr seasonal cycle experiment with CCM1 at R15. Thick solid line represents 200-m contour of CCM1 representation of Antarctic ice sheet.

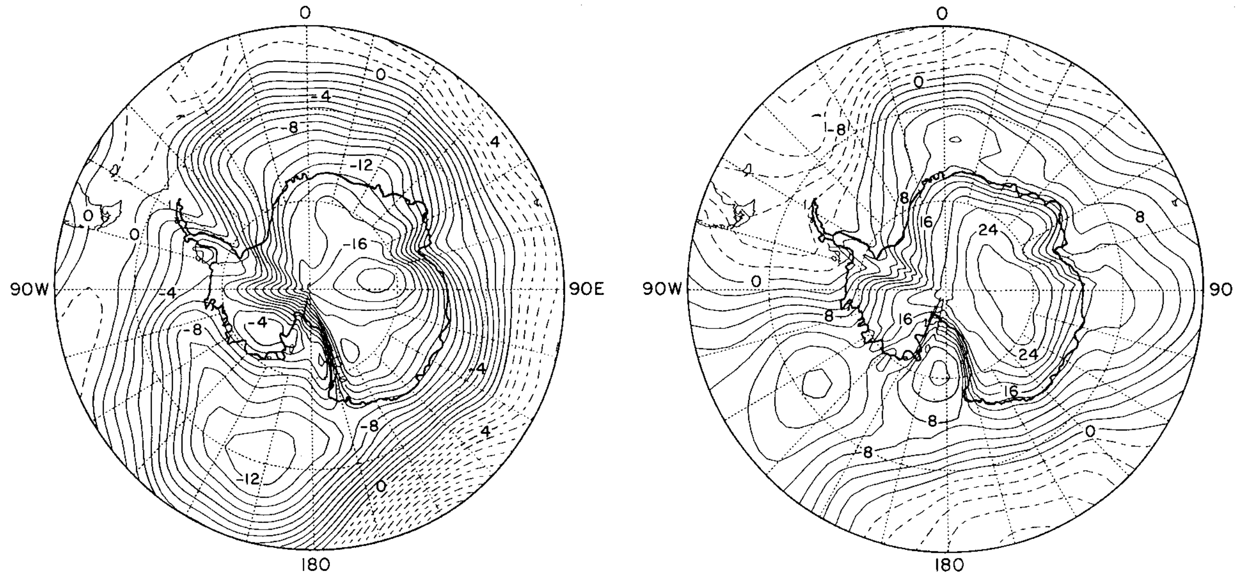

FIG. 3. Mean monthly surface pressure differences. April minus January 1987 (left) and December minus September 1990 (right) based on ECMWF analyses.

pear to follow the contours of the model terrain so precisely that the resolution difference between the coarse CCM1 (approximately 4.5° latitude by 7.5° longitude) and the finer-scale ECMWF (2.5° by 2.5°) depiction of the Antarctic orography is obvious. Note that even gradients in the ice topography are mirrored with a high degree of fidelity in the gradients of seasonal surface pressure change.

Austral springtime and autumn are periods of rapid and dramatic changes in the Antarctic atmosphere. The influence of solar insolation is paramount to observed seasonal changes. Mean sounding data from Antarctic interior stations Vostok and South Pole for the years 1973–92 indicate a 30-hPa temperature increase of approximately 40°C from September to December followed by 30°C decrease from January to April. Zonal wind components in the polar stratosphere undergo profound change during these periods as well. At the coastal station Davis (68.6°S, 78.0°E), mean 20-yr 30-hPa zonal wind components decrease by over 100 m s^{-1} from September to December, and the strong cyclonic circulation of late winter about the continental periphery becomes transformed into a weak anticyclonic circulation by early summer.

Large changes also take place at the surface. The solar heating of the sloping Antarctic terrain during the austral

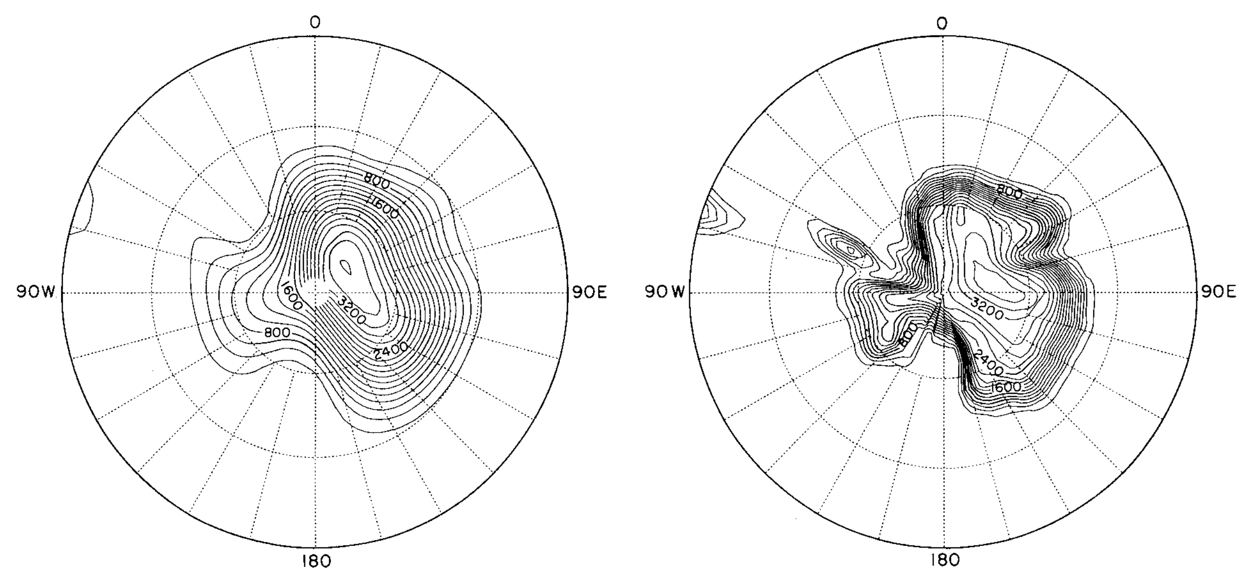

FIG. 4. Representations of Antarctic ice topography in CCM1 (left) and ECMWF (right). Contour lines in m.

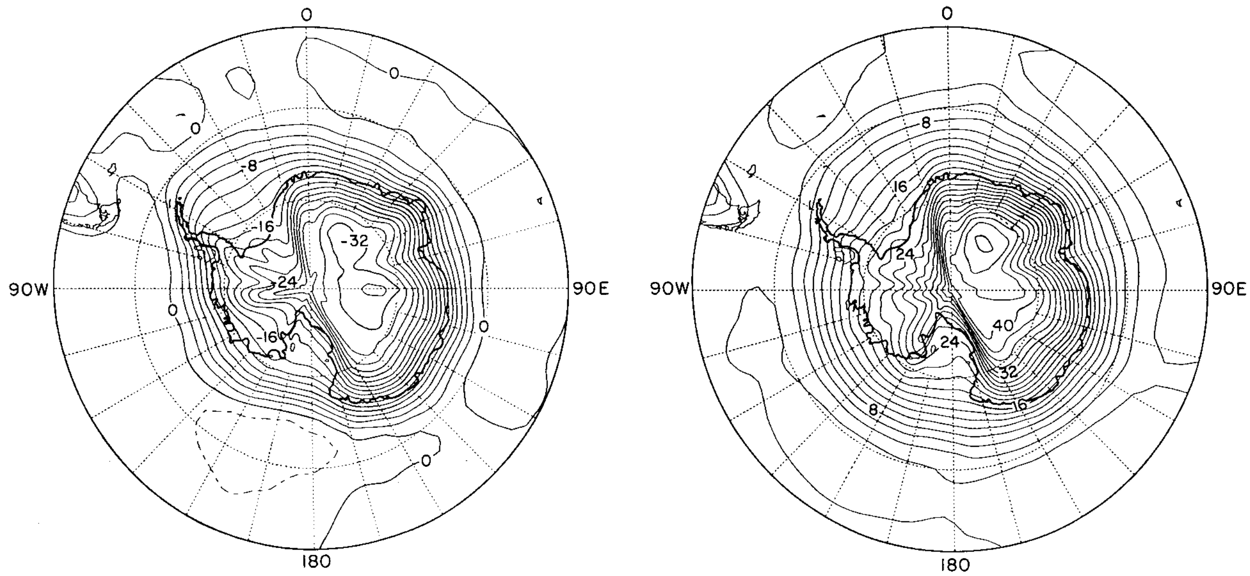

FIG. 5. Mean monthly surface temperature differences. April minus January 1987 (left) and December minus September 1990 (right) based on ECMWF analyses.

springtime produces a zonally averaged temperature increase in excess of 20°C based on results of a 5-yr seasonal cycle CCM1 simulation (Parish et al. 1994). Likewise, the rapid onset of winter from January to April results in a zonally averaged cooling of the CCM1 ice slopes of approximately 20°C. The temperature changes are even more pronounced at individual interior stations such as at the Dome C site. Mean monthly temperatures decrease by 40°C from January to April during some years (Keller et al. 1994). Figure 5 depicts the corresponding changes in the mean monthly ECMWF surface temperatures for the transitional periods January–April 1987 (Fig. 5a) and September–December 1990 (Fig. 5b) shown in Fig. 3. In both cases, the temperature change patterns again display an unmistakable coherency with the ECMWF orography. The greatest changes are again situated over the east Antarctic interior.

The isallobaric patterns illustrated in Figs. 2 and 3 are unquestionably related to the seasonal diabatic heating cycle and resulting net mass transports. Figure 6 illustrates in cross-sectional form the zonally averaged temperature changes from January to April 1987 (Fig. 6a) and September to December 1990 (Fig 6b). In both cases, strong modification is present over the Antarctic ice slopes as well as in the stratosphere. Zonally averaged surface temperatures decrease during the austral autumn 1987 period in excess of 20°C from 72°S to the South Pole. Significant temperature decreases can be traced into the upper troposphere; a January–April 1987 temperature decrease of 8°C is present at 400 hPa over much of Antarctica. Surface temperature changes accompanying the austral springtime transition in 1990 are even larger. Hydrostatic considerations dictate that as the temperature of the atmospheric column adjusts to the changing solar insolation, the distribution of pressure with height becomes modified in a corresponding manner. The thickness between two isobaric levels is proportional to temperature. For example, assuming that the sea level pressure remains constant, a mean column temperature decrease from 260 K to 240 K implies that at an elevation of 3000 m the pressure would decrease by approximately 20 hPa. This is the magnitude of surface pressure change observed on the high plateau of Antarctica. Through such hydrostatic arguments, it is expected that isallobaric tendencies seen during both austral autumn and springtime would mirror the topographic contours of Antarctica.

It is impossible to decouple the atmospheric thermodynamics and dynamics, especially in the lowest levels of the troposphere over the Antarctic ice terrain. The radiational cooling of the sloping ice fields during austral autumn results in the establishment of a horizontal pressure gradient force directed downslope. This acceleration leads to the development of the much-heralded katabatic wind regime, which transports vast amounts of cold, negatively buoyant air northward from Antarctica. The rapid austral autumn cooling results in a concurrent intensification of the continental katabatic wind pattern (e.g., Parish 1992a,b; Bromwich et al. 1993). At Terra Nova Bay (74.6°S, 163.4°E), situated on the steep terminus of the Antarctic ice slope, wind speeds increase by a factor of 2 in less than a month from late February to mid-March (Bromwich 1989; Parish 1992a; Bromwich et al. 1993) with an almost equally impressive decline during the early summer months from mid-October to December. We propose that the near-surface thermodynamics and attendant slope flows are the fundamental forcing agents in the austral autumn surface pressure changes over Antarctica. However, we

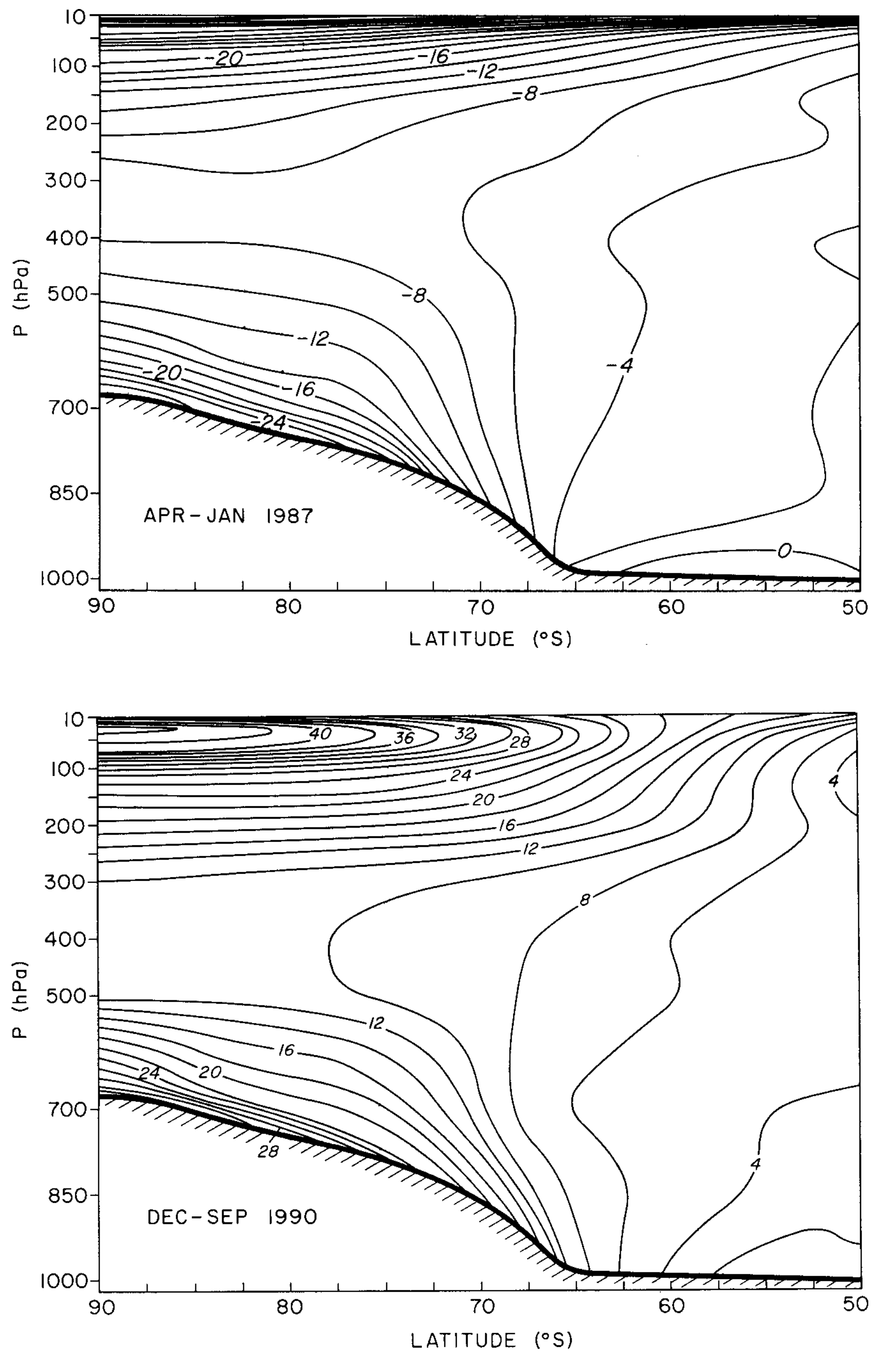

FIG. 6. ECMWF zonally averaged cross section of temperature changes. April minus January 1987 (top) and December minus September 1990 (bottom).

speculate that the rapid stratospheric adjustments during the austral springtime result in a broad overturning and hence a resulting surface pressure change signal that encompasses most of Antarctica. The difference in the magnitude between the austral springtime and autumn surface pressure changes is probably due to the stratospheric influence.

The organized nature of the isallobaric pattern over Antarctica as illustrated in Figs. 2 and 3 suggests that a mean meridional transport is present over a broad portion of the Southern Hemisphere (SH) stretching from the polar regions to the subpolar latitudes during the austral autumn and springtime periods. The phase of the isallobaric signal reverses between 50° and 60°S, which, from continuity arguments, implies a mass exchange across this latitude belt. This also suggests a

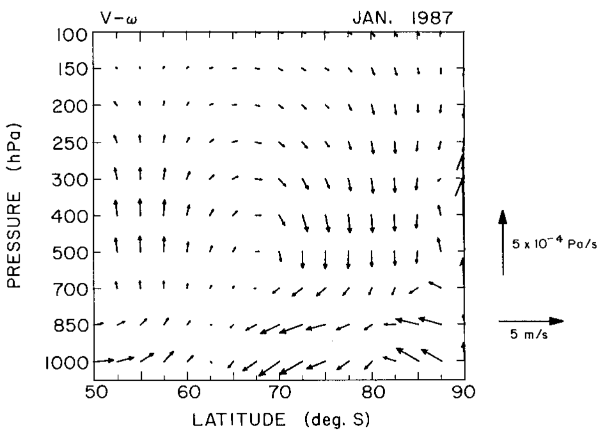

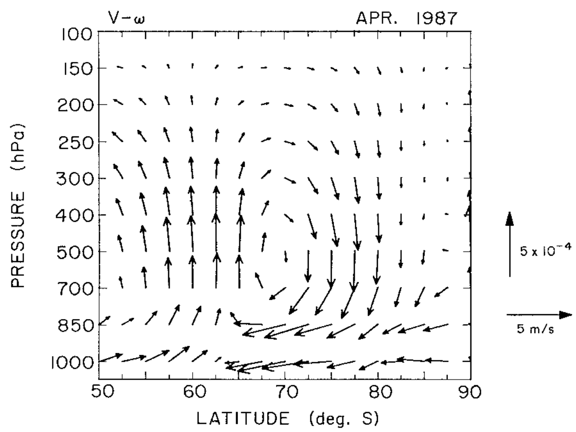

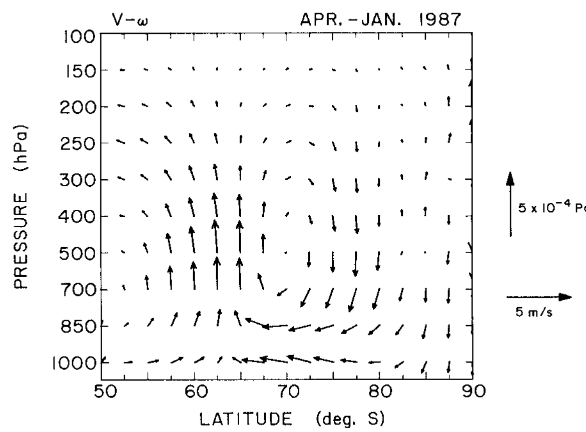

FIG. 7. ECMWF zonally averaged cross section of meridional and vertical velocity components on isobaric levels for (a) January 1987, (b) April 1987; ECMWF zonally averaged cross section of meridional and vertical velocity differences April 1987 minus January 1987 are shown in (c). Surface values have been extrapolated downward through the ice sheet over Antarctica.

direct connection between Antarctica and the middle latitudes of the SH that has no Northern Hemisphere counterpart. The Antarctic orography is thought to play a fundamental role in the mean meridional circulation and mass transport at high southern latitudes. Egger (1985), James (1989), and Parish (1992a) have considered the impact of the radiative cooling of the Antarctic ice slopes and attendant katabatic wind regime on the large-scale circulation in the high southern latitudes. They note that a thermally direct meridional circulation becomes established between Antarctica and the subpolar latitudes. The low-level katabatic drainage off the high plateau of Antarctica represents a significant component of the lower branch of the meridional circulation (see also Parish et al. 1994). Continuity requirements force a broad southward-directed return branch at upper levels of the troposphere and a general subsidence over the continent that feeds the katabatic layer.

The continental-scale katabatic wind regime is sensitive to the seasonal cycle of solar insolation. This implies that the mean meridional circulation between Antarctica and more northerly latitudes undergoes a seasonal modulation with the largest changes taking place near the surface. Conceptually, the diabatic modulation of the lower branch of the thermally direct circulation can be envisaged as resulting in a temporal imbalance in the net mass flux over the continent. During the austral autumn, intensification of the katabatic wind regime and hence lower branch of the meridional circulation occurs; a net mass transport away from the continent will initially result. During the austral springtime, the reduction of the katabatic wind transport at low levels implies that the poleward transport in the middle and upper troposphere as well as the lower stratosphere will dominate for a short period of time and a mass loading onto the continent will occur. Such a conception of the mean meridional circulation is no doubt highly simplified but is consistent with the observed surface pressures.

To illustrate the seasonal modulation of the mean meridional circulation, depiction of the mean monthly circulations have been prepared. The standard ECMWF output set utilized includes state parameters interpolated to standard isobaric levels. Figure 7 illustrates the ECMWF mean meridional circulation for the 1987 austral autumn case. During January 1987 (Fig. 7a), a weak thermally direct meridional circulation over Antarctica is depicted. By April 1987 (Fig. 7b) the low-level outflow, reflecting primarily the katabatic wind regime, has strengthened significantly and the mean meridional cir-

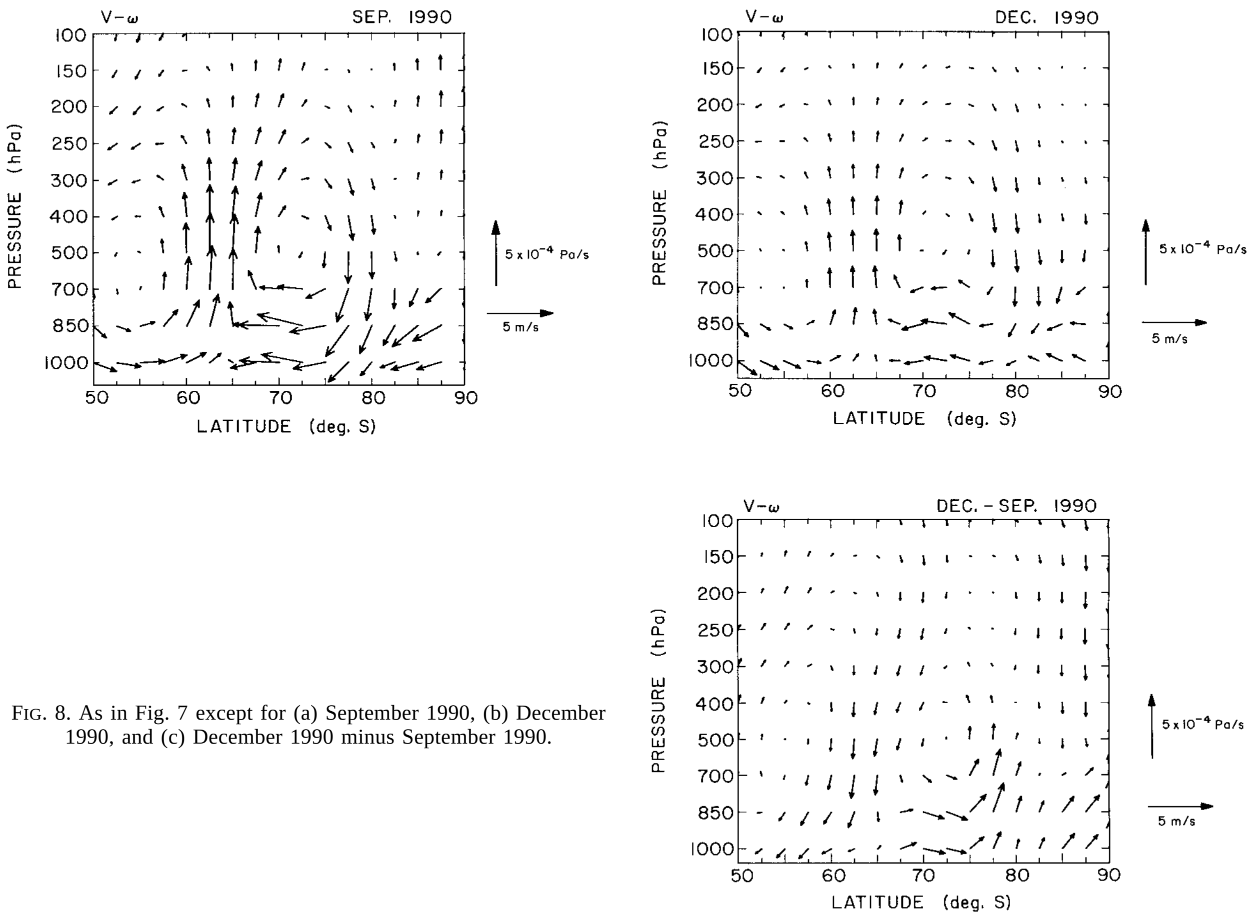

FIG. 8. As in Fig. 7 except for (a) September 1990, (b) December 1990, and (c) December 1990 minus September 1990.

culation has become more pronounced. Figure 7c illustrates the differences in the mean meridional circulation between April and January of 1987. The intensification of the lower branch of the mean meridional circulation is apparent. From the available ECMWF datasets, it is not possible to determine accurately the mass budgets so as to permit calculation of accurate surface pressure tendencies. However, it is clear that the changes in the meridional circulation support a transfer of atmospheric mass away from Antarctica and surface pressure falls over the continent.

By contrast, Fig. 8 illustrates the mean meridional circulation for the austral springtime case of September (Fig. 8a) and December (Fig. 8b) 1990. The decrease in the intensity of the lower branch of the mean meridional circulation is apparent. The difference in the mean meridional circulation (Fig. 8c) reflects the weakening of the katabatic outflow. Changes in the upper-level meridional components are again considerably smaller than those seen at low levels. The vector difference in the mean meridional circulation from September to December suggests that the low-level decreases in the intensity of the outflow are again the largest changes. There is a suggestion that the upper-level branch, especially the southward-directed component, does not experience similarly large changes. Thus, the upper-level mass inflow (including the stratospheric component) appears to be dominant over the rapidly weakening low-level outflow during this period, and surface pressures over the continent display a significant increase. The net seasonal surface pressure changes can be envisaged as a result of the adjustment process by which low-level temperature and katabatic wind regimes attempt to attain a quasi-balanced state in response to changing solar insolation.

3. Numerical simulations of katabatic winds

a. Overview

As a means of testing the hypothesis that diabatic processes at the surface are responsible for the observed surface pressure falls during austral autumn, use of a numerical model has been employed. Numerical simulations presented will focus on the onset of the katabatic wind, in which the process of diabatic cooling of the terrain is the sole forcing mechanism for mass redistribution. The simulation is taken as illustrative of atmospheric changes associated with the rapid onset of the katabatic wind regime during the austral autumn period. The ability to isolate the diabatic cooling process allows a direct evaluation of the importance of the thermodynamical–dynamical interactions over the sloping Antarctic ice fields on the surface pressure tendency.

The model used is a modified version of that described by Anthes and Warner (1978), which has been used extensively to study Antarctic drainage flows. A description of the model including the relevant equations can be found in Parish and Waight (1987). The model is written in sigma coordinates to allow for inclusion of irregular terrain. A total of 15 vertical levels is used in the model (σ = .998, .99, .98, .97, .96, .94, .92, .90, .85, .775, .70, .60, .50, .30, .10); the pressure at the top of the model is 250 hPa. The high resolution in the lower levels of the atmosphere is necessary to depict the katabatic wind. The lowest sigma level corresponds to a height of approximately 11 m above ground level. The model incorporates a graybody longwave radiation scheme following Cerni and Parish (1984) that allows calculation of radiative fluxes at the various sigma levels in a moderately efficient manner. For the numerical experiments presented, radiative cooling at the surface is the driving mechanism for the katabatic wind regime. A surface energy budget based on the force–restore model of Blackadar (1978) is used to depict changes in temperature at the ice surface; turbulent fluxes of heat and momentum within the surface boundary layer are modeled using similarity theory (Businger et al. 1971). An explicit representation of the planetary boundary layer is attempted. Turbulent fluxes are evaluated using a first-order closure scheme in which the eddy diffusivity values are determined using the equations proposed by Brost and Wyngaard (1978). The specification of the height of the planetary boundary layer is also taken from that work. This set of parameterizations ensures a natural evolution of the katabatic wind interaction with the large-scale environment.

b. Two-dimensional simulations

Although the high plateau region of east Antarctica is displaced nearly 10° from the South Pole, the continent can be assumed to be axisymmetric. The east Antarctica coastline runs roughly along the 68°S parallel from 10°W to nearly 180° longitude. A steep coastal escarpment is present throughout this section of Antarctica. The large-scale drainage patterns over east Antarctica as illustrated in Parish and Bromwich (1987) suggest that the axisymmetric assumption is acceptable as a first-order approximation. All 2D model equations have been modified to allow for this assumption.

Here we follow Parish and Waight (1987) and use a power law fit to obtain a representative terrain profile for a section of east Antarctica,

$$z = 4000.0(1 - r/2.0 \times 10^6)^{0.45},$$

where z is the terrain height in meters at a distance r in meters from the center of the ice plateau. The model simulations employ a horizontal grid of 80 points with a grid spacing of 20 km. The terrain slopes as represented in the model vary from slightly less than 0.002 in the interior to approximately 0.04 at the coast. Such values are representative of observed ice slopes over the continent.

The model results to be discussed are based on 10-day simulations of Antarctic katabatic winds at the start of the austral winter in which no solar radiation is assumed to fall on the ice sheet. The timescale of the integration is sufficient to illustrate the adjustment process accompanying the development of the winter katabatic wind regime. The impulsive nature of the cooling ensures that the adjustment from the summer to winter katabatic wind regime will require a considerably shorter timescale than that suggested by observations.

Initially, the Antarctic atmosphere is assumed to be at rest with no horizontal pressure gradients present throughout the model domain. Thus, no synoptic-scale forcing is present in the simulation; all motion is therefore derived from the radiative cooling of the sloping ice surface and subsequent evolution of the katabatic wind regime. Such flat pressure fields are assumed representative of the horizontal pressure gradients found during the austral summer over the Antarctic continent. An initial temperature field in the free atmosphere was taken from the Byrd station mean January sounding shown in Schwerdtfeger (1984, see his Fig. 6.9). The thermal structure at the start of the model run is without a surface inversion and is assumed to be representative of nonkatabatic wind events at the end of the austral summer. The ocean to the north of the Antarctic continent is assumed to be covered with a solid ice shelf and exhibits continental characteristics.

As the pronounced radiative flux divergence at the surface cools the sloping ice terrain during the first couple hours of model integration, the katabatic wind regime begins to develop. With the intensification of the near-surface drainage flows, the turbulent exchanges in the surface boundary layer increase. The turbulent transfer enhances the cooling of the lower atmosphere, which then allows the katabatic flow to reach higher levels. The intensity of the katabatic wind regime reaches a maxima within the first twelve hours or so. The strongest drainage flows are found at the coastal grid point where the terrain slopes are steepest. Maximum drainage wind intensities reach a speed of nearly 14 m s^{-1}. Figure 9 illustrates the 10-day evolution of the katabatic wind speeds and wind directions in 1-day increments at the first sigma level. Note that the wind speeds over the continental interior show a monotonic increase from the high plateau to the coast (Fig. 9a). An abrupt decrease in the katabatic wind intensity occurs as the drainage current moves offshore over the flat ice-covered ocean. Note that the drainage flows can be traced out several hundred kilometers at day 2. The low-level mass convergence north of the steep coastal margin induces rising motion in the band adjacent to the continent. This branch

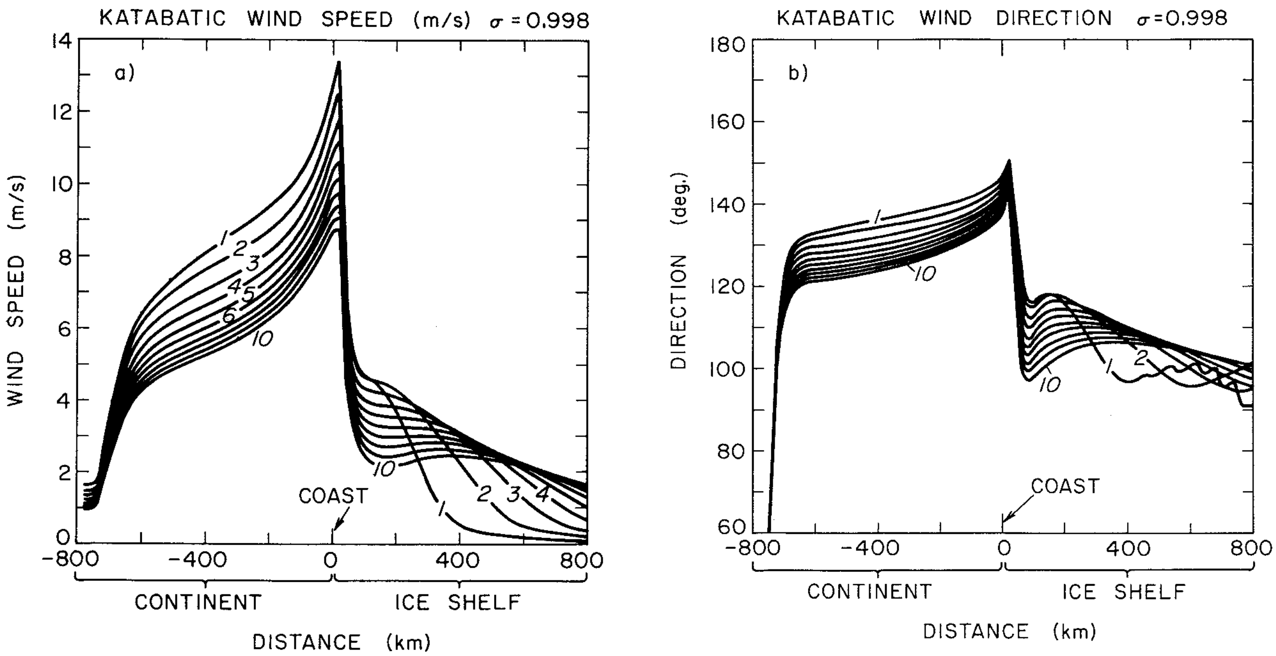

FIG. 9. Numerically simulated 10-day evolution of (a) wind speed and (b) wind direction at $\sigma = .998$ (approximately 11 m above ground) from two-dimensional model experiment.

of rising motion represents the northern edge of the mean meridional circulation forced by the katabatic wind regime.

Katabatic wind intensity steadily decreases throughout the 10-day period similar to that shown in Parish (1992a). A mean meridional circulation becomes established due to the developing thermal contrast and attendant katabatic wind regime. The induced upper-level mass convergence over the Antarctic continent, necessary to resupply the low-level katabatic regime, generates cyclonic vorticity in the middle to upper troposphere. The adverse horizontal pressure gradients associated with the developing vortex act to suppress the katabatic wind regime. In the limiting case, the katabatic wind regime is responsible for its own demise. Egger (1985, 1992) and James (1988, 1989) have noted that the real atmosphere must somehow rid itself of the cyclonic vorticity since observations do not show a pronounced decline with time of the katabatic wind intensity. Recently, Juckes et al. (1994) have noted that a balance between the Eliassen–Palm flux convergence and Coriolis torque dominates the momentum budget over Antarctica. However, the coastal katabatic wind speeds compare favorably with observations from katabatic-prone stations along the coast of Antarctica during the entire model integration period.

The katabatic winds are directed from 30° to 50° to the left of the fall line (oriented at 180° in Fig. 9b), consistent with Coriolis deflection of pure slope flows. The coastal katabatic wind is directed mostly downslope with a deviation angle of approximately 30° from the fall line at day 2. Drainage flows over the interior reflect near-geostrophic conditions with wind directions approaching 60° from the fall line. Marked directional change takes place just north of the terminal slopes of the coast. Wind directions back suddenly by 30°, changing from predominantly southerly to a more easterly direction. This change is brought about by pseudoinertial turning of the katabatic airstream as it outruns the supporting horizontal pressure gradients over the sloping ice terrain. Predominantly easterly flows are found in the near-surface layer over the entire ice-covered ocean to the north of the continent. This matches the observed circumpolar band of easterlies that is found just north of the continental coastline.

The mean meridional circulation induced by the surface radiational cooling and attendant katabatic wind regime significantly alters the mass and wind fields throughout the troposphere in the high southern latitudes. It is through this thermally direct latitudinal exchange that the influence of the radiational cooling of the surface and attendant katabatic wind regime are conveyed to the ambient atmosphere over Antarctica. Figure 10 illustrates the surface pressure change at 1-day increments accompanying the evolution of the katabatic wind regime. The largest pressure changes take place during the first few days and are maximized over the high interior of the continent. Surface pressures drop rapidly over the high interior in excess of 3 hPa day^{-1} in response to the cooling of the sloping ice terrain. This mass is being removed via the katabatic wind outflow in the lowest few hundred meters of the atmosphere. The scale of this pressure change is reasonable by simple budget estimates. Katabatic winds with a meridional

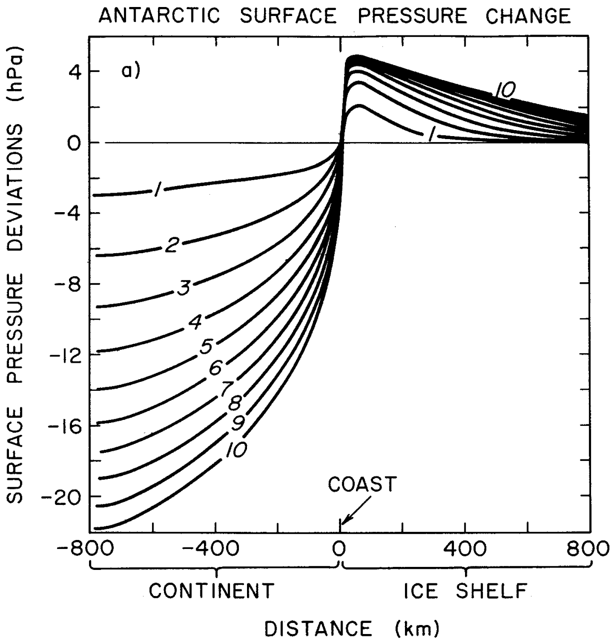

FIG. 10. Surface pressure changes from start of two-dimensional model experiment over idealized Antarctic region.

component of 10 m s^{-1} over a depth of 100 m across the 70° latitude circle alone will result in a 9 hPa pressure decrease per day over the interior of the continent. Obviously, compensating motions become established in the middle to upper troposphere that moderate the net pressure change. Note that the profile of pressure change over the idealized Antarctic continent takes on the characteristic shape of the underlying terrain with the largest pressure decrease situated over the high plateau. Similar to that seen in Figs. 2 and 3, the model-simulated isallobaric contours accompanying the katabatic wind development match the contours of the ice topography.

The pattern of surface pressure changes also reflects the radiational cooling of the near-surface layers. Note that at the coastal grid point, surface pressures display little change over the course of the model integration. Hydrostatic considerations imply that the cooling in the lowest layers of the atmosphere must result in a more rapid pressure change with height and hence surface pressure changes over the ice sheet that increase with terrain height. Figure 11 depicts the temperature changes during the 10-day integration period. It can be seen that the largest temperature decrease occurs at the surface where decreases of 25°C or greater are found. The cooling is seen to extend through a significant portion of the troposphere over Antarctica. The magnitude of the temperature change is similar to the seasonal decrease illustrated in Fig. 6a, except for the region to the north of the continent and at the highest levels. The numerical simulation shows that the low levels over the oceanic section to the north of the continent display the largest temperature decrease of near 30°C during the 10-day integration period. The ECMWF analyses suggests little temperature change during the austral autumn period. This marked difference is a result of the solid ice shelf assumed in the model simulation. Physically, the model results should be expected. Automated

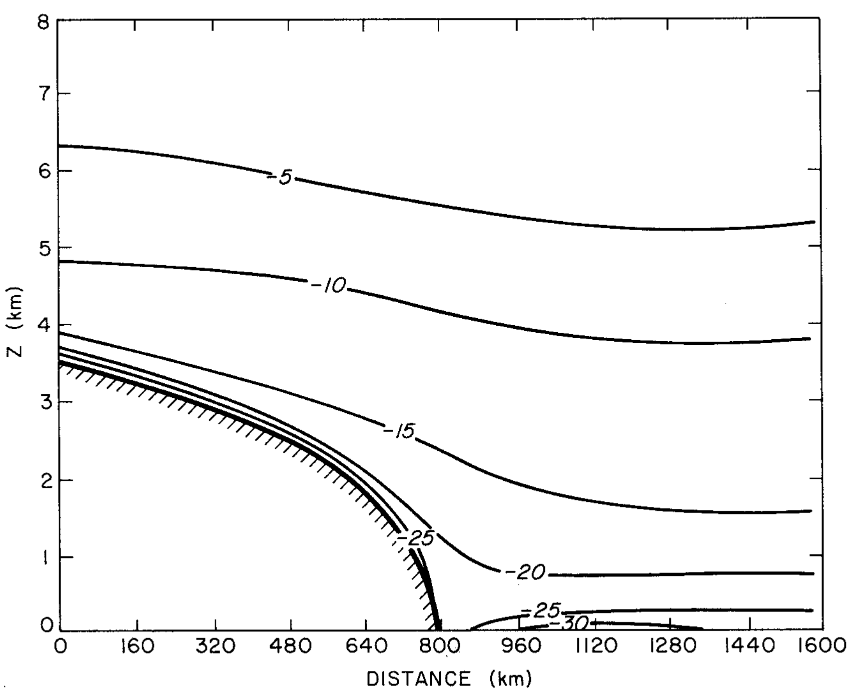

FIG. 11. Cross section of 2D model-simulated 10-day temperature change (°C).

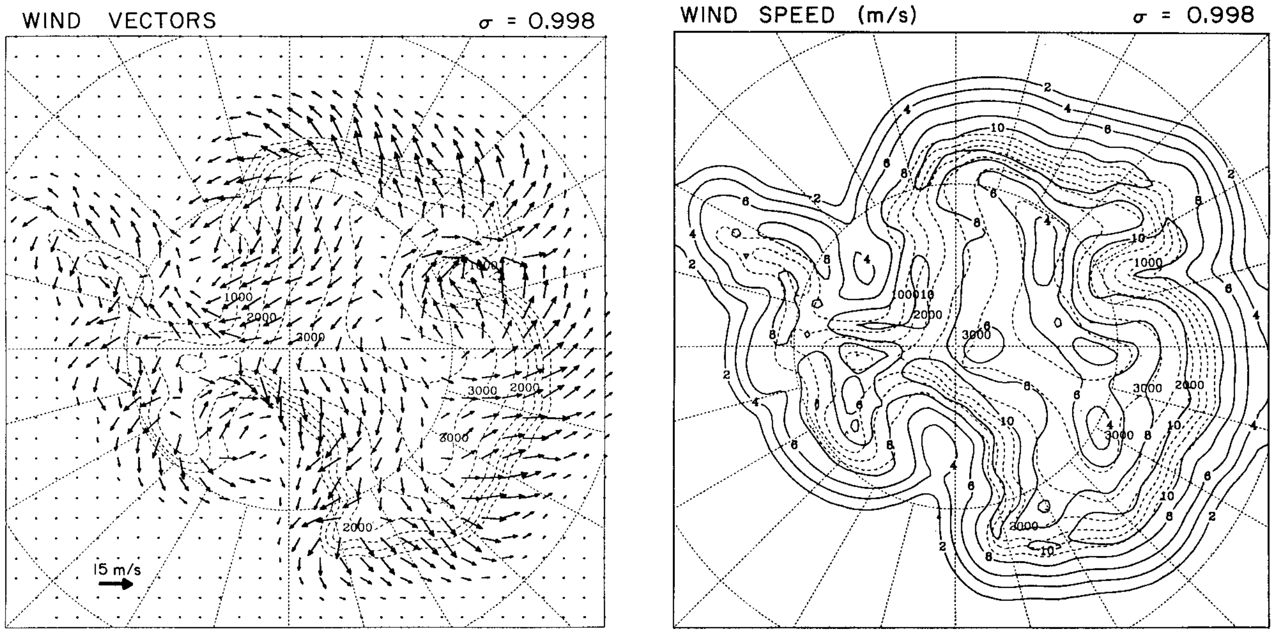

FIG. 12. Three-dimensional simulation of (a) wind vectors and (b) wind speeds at $\sigma = .998$ (approximately 11 m) after 2 days of model integration.

Weather Station observations suggest that the coldest potential temperatures in the Antarctic are found on the Ross Ice Shelf. The second major difference is in the stratosphere where the ECMWF analyses suggest a large cooling. The model domain only considers the troposphere with a top level of 250 hPa.

There is a strong interplay between the thermodynamics and dynamics during this 10-day model simulation. It is apparent from hydrostatic considerations that the colder temperatures in the lower portion of the troposphere are required for the more rapid pressure decrease with height over the Antarctic ice massif. However, it is the katabatic wind field that is the transport agent for removing the mass from the Antarctic continent. This symbiosis as seen in the model is thought to represent accurately the physical processes at work during the austral autumn period. This emphasizes the first order importance of the terrain-induced processes in modification of the ambient pressure field.

c. Three-dimensional simulations

Two-dimensional numerical simulations clearly show that the drainage flows are potentially important in redistributing mass about the high southern latitudes. To explore the influence of the katabatic wind on the mass distribution over the entire continent, three-dimensional numerical experiments have been performed. Results of one 10-day integration will be presented here. Again, we argue that the impulsive cooling process in the model simulations accelerates the winter adjustment process and the results of the surface pressure change simulations over Antarctica should be representative of the onset of the winter katabatic wind regime. The model is identical to the two-dimensional version except for the horizontal grid (60×60) and grid spacing that was set to 100 km to capture the entire Antarctic orography. Previous experiments (Parish and Bromwich 1991) have shown that this resolution is adequate to depict details of the drainage flow over the continent such as displayed in Parish and Bromwich (1987). The model was again initialized with a motionless atmosphere, and the simulations have assumed polar night conditions.

As in the two-dimensional case, the drainage winds form rapidly due to the cooling of the terrain slopes. The intensity of the coastal katabatic wind regime is somewhat weaker than in the two-dimensional case since the 100-km resolution considerably smooths the terminal coastal ice slopes. Nevertheless, the resulting drainage flow regime after 2 days of model integration (Fig. 12a) is nearly identical to the depiction in Parish and Bromwich (1987, 1991). Once the drainage flows develop, the streamline pattern of the katabatic wind over the continent (not shown) remains essentially identical throughout the simulation. The near-surface wind vectors display a radial drainage pattern off the elevated ice domes of East Antarctica, with wind speeds (Fig. 12b) reaching a maximum of approximately 12 m s^{-1} along the coastal stretches. The intensity of the coastal katabatic wind over East Antarctica decreases slightly less rapidly with time than that suggested by the 2D simulations. The 10-day wind speeds at the lowest sigma level are approximately 75% of the 2-day values. Confluence is noted near the coast along approximately 70°E, 140°E, and the western portions of the Ross and Weddell Seas.

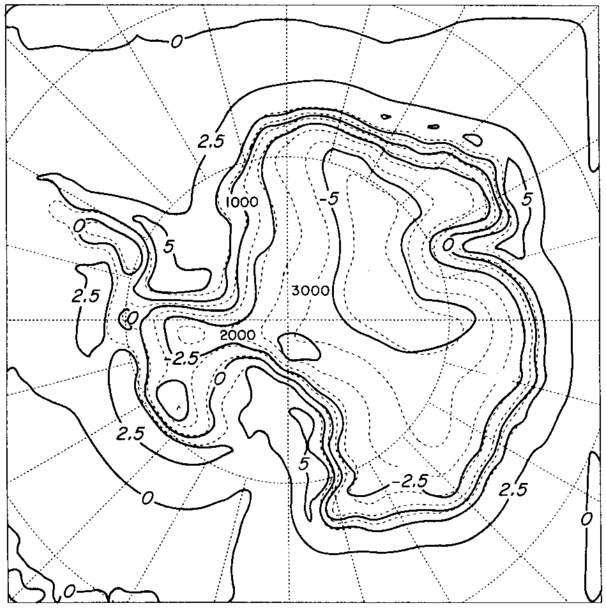

FIG. 13. Surface pressure changes (hPa) from start of three-dimensional model experiment after 2 days of model integration.

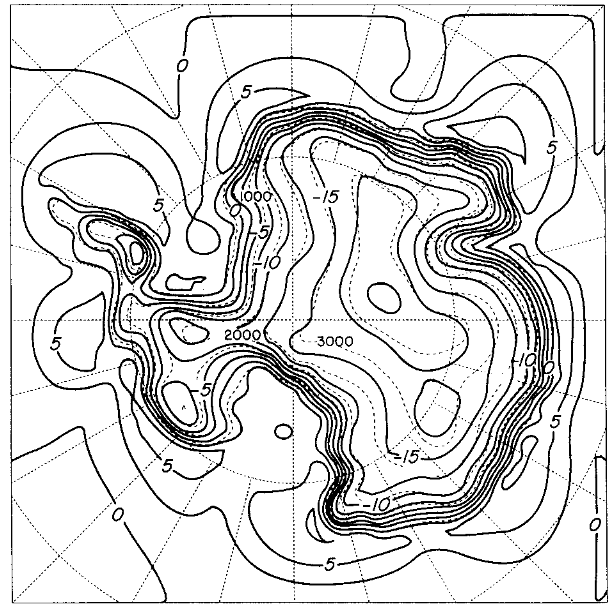

FIG. 14. As in Fig. 9 except for 10 days of model integration.

Figure 13 illustrates the surface pressure change at day 2 accompanying the katabatic wind development. Surface pressure decreases are maximized over the highest portion of the East Antarctic plateau and exceed 7 hPa. In general, the pressure falls are slightly less than seen in the 2D model simulations. However, note that the isallobaric pattern again appears tied to the continental orography. This atmospheric mass adjustment over Antarctica is characteristic of the diabatic cooling of the lower atmosphere and development of the katabatic wind circulation. As seen in the ECMWF 1987 austral autumn analyses, the isallobars mirror the terrain contours almost exactly, with the strongest isallobaric gradient found over the steep coastal slopes.

North of the continent over the ice shelf, by day 2 surface pressures have risen by up to 5 hPa in response to the deceleration of the katabatic airstream and attendant piling up of mass just offshore from the continent. This mass change over the offshore environment results in a pressure gradient force that supports a well-defined circumpolar easterly low-level wind regime. There seems no doubt that in the real atmosphere transient extratropical cyclonic disturbances, which are found frequently in a circumpolar band to the north of Antarctica, play a major role as well in the observed sea level low pressure regime. Schwerdtfeger (1984, 139), among others, has pointed out that the climatologically observed sea level low pressure band encircling the continent is the site of maximum cyclonic activity. He estimates that the mean position of the low pressure belt is approximately 62°S north of the East Antarctic coast between 30°E and 150°E, which is roughly 500 km beyond the Antarctic coastline. The scale of the simulated offshore surface pressure gradient that can be inferred from Fig. 13, however, is consistent with the climatological average.

This isallobaric pattern continues over the Antarctic continent as the integration proceeds. At day 5, surface pressures over the interior of the continent have dropped by approximately 15 hPa since the start of the model integration. Again, the isallobaric pattern follows the topographic contours of Antarctica with moderate isallobaric gradients over the interior ice slopes and sharp gradients of the pressure tendency over the steeply sloping coastal ice topography. At the end of the 10-day integration period, surface pressures over the continent (Fig. 14) have dropped in excess of 20 hPa and the surface pressure changes associated with the continued cooling of the ice surface and attendant katabatic drainage remain intimately linked to the underlying surface.

4. Summary

Results presented in the previous section show that the radiative cooling and concomitant katabatic wind regime over Antarctica are responsible for the establishment of a mean meridional circulation over the high southern latitudes. Mass convergence offshore from Antarctica is responsible for the movement of warmer, subpolar air towards Antarctica at middle to upper tropospheric levels. During the transitional periods January–April and September–December, it has been proposed that the lower branch of the mean meridional circulation becomes modulated significantly by the rapidly changing solar radiation reaching the Antarctic ice slopes. Hence, seasonal changes in the atmospheric mass loading over the continent occur. Such surface pressure changes are required because of the rapidly changing thermodynamic structure over the high southern latitudes and resulting modification in the horizontal pressure field over Antarctica. This underscores the strong interplay between atmospheric dynamics and thermodynamics over the sloping Antarctic ice fields and the importance of this interaction on the mean meridional circulation over the continent. The nature of the mass adjustment portrayed by the numerical simulations matches the spatial patterns displayed by the observed isallobaric contours illustrated in Figs. 2 and 3, and the magnitude of the austral autumn surface pressure change scales well with observations.

We argue that the simulated adjustment process accompanying the development of the katabatic wind regime is fundamentally the same as in the real atmosphere during the austral autumn period. The length of the integration period is not particularly sensitive. Extended integration periods of 20 days have been completed that show only slightly larger isallobaric values. Without question, the most pronounced adjustment in the numerical experiments occurs within the first 10-day period. It is obvious that the impulsive, idealized nature of the model simulations forces the adjustment process to proceed at an accelerated timescale as compared to the actual situation. Superimposed, of course, will be changes in pressure brought about by synoptic-scale and longer-term transient systems, which can modify to some extent the pattern of observed surface pressure changes. Although we do not present model simulations of the austral springtime case, we speculate that similar arguments hold that explain in large part the rapid pressure rise during that period. Such seasonal mass adjustment over Antarctica must play a critical role in forcing the annual cycle of pressure over the high southern latitudes. It also seems likely that the mass transports associated with such atmospheric mass loading over Antarctica play a role in the semiannual oscillation.

Acknowledgments. This work was supported in part by NASA through Grants NAGW-2666 to TRP and NAGW-2718 to DHB and by the National Science Foundation through Grants DPP-9117202 and DPP-9218544 (TRP). The CCM1 simulations were performed on the Cray Y-MP of the Ohio Supercomputer Center, which is supported by the state of Ohio. Automatic weather station data were provided by Charles R. Stearns at the University of Wisconsin—Madison through Grants NSF-DPP 86-06385, 88-18171, and 90-15586.

REFERENCES

Anthes, R. A., and T. T. Warner, 1978: The development of hydrodynamical models suitable for air pollution and other mesometeorological studies. *Mon. Wea. Rev.,* **106,** 1045–1078.

Blackadar, A. K., 1978: High resolution models of the planetary boundary layer. *Advances in Environmental and Scientific Engineering,* Vol. 1, Gordon and Breach, 51–85.

Bromwich, D. H., 1989: An extraordinary katabatic wind regime at Terra Nova Bay, Antarctica. *Mon. Wea. Rev.,* **117,** 688–695.

——, T. R. Parish, A. Pellegrini, C. R. Stearns, and G. A. Weidner, 1993: Spatial and temporal characteristics of the intense katabatic winds at Terra Nova Bay, Antarctica. *Antarctic Meteorology and Climatology: Studies Based on Automatic Weather Stations,* D. H. Bromwich and C. R. Stearns, Eds., Antarctic Research Series, Vol. 61, Amer. Geophys. Union, 47–68.

Brost, R. A., and J. C. Wyngaard, 1978: A model study of the stably-stratified planetary boundary layer. *J. Atmos. Sci.,* **35,** 1427–1440.

Businger, J. A., J. C. Wyngaard, Y. Izumi, and E. F. Bradley, 1971: Flux-profile relationships in the atmospheric surface layer. *J. Atmos. Sci.,* **28,** 181–189.

Cerni, T. A., and T. R. Parish, 1984: A radiative model of the stable nocturnal boundary layer with application to the polar night. *J. Climate Appl. Meteor.,* **23,** 1563–1572.

Egger, J., 1985: Slope winds and the axisymmetric circulation over Antarctica. *J. Atmos. Sci.,* **42,** 1859–1867.

——, 1992: Topographic wave modification and the angular momentum balance of the Antarctic troposphere. *J. Atmos. Sci.,* **49,** 327–334.

James, I. N., 1988: On the forcing of planetary-scale Rossby waves by Antarctica. *Quart. J. Roy. Meteor. Soc.,* **114,** 619–637.

——, 1989: The Antarctic drainage flow: Implications for hemispheric flow on the Southern Hemisphere. *Antarct. Sci.,* **1,** 279–290.

Juckes, M. N., I. N. James, and M. Blackburn, 1994: The influence of Antarctica on the momentum budget of the southern extratropics. *Quart. J. Roy. Meteor. Soc.,* **120,** 1017–1044.

Keller, L. M., G. A. Weidner, and C. R. Stearns, 1994: Antarctic automatic weather station data for the calendar year 1992. Department of Atmospheric and Oceanic Sciences, University of Wisconsin—Madison, 356 pp. [Available from Department of Atmospheric and Oceanic Sciences, University of Wisconsin—Madison, Madison, WI 53706.]

Meehl, G. A., 1991: A re-examination of the mechanism of the semiannual oscillation in the Southern Hemisphere. *J. Climate,* **4,** 911–926.

Parish, T. R., 1992a: On the interaction between Antarctic katabatic winds and tropospheric motions in the high southern latitudes. *Aust. Meteor. Mag.,* **40,** 149–167.

——, 1992b: On the role of Antarctic katabatic winds in forcing large-scale tropospheric motions. *J. Atmos. Sci.,* **49,** 1374–1385.

——, and D. H. Bromwich, 1987: The surface windfield over the Antarctic ice sheets. *Nature,* **328,** 51–54.

——, and K. T. Waight, 1987: The forcing of Antarctic katabatic winds. *Mon. Wea. Rev.,* **115,** 2214–2226.

——, and ——, 1991: Continental-scale simulation of the Antarctic katabatic wind regime. *J. Climate,* **4,** 135–146.

——, D. H. Bromwich, and R.-Y. Tzeng, 1994: On the role of the Antarctic continent in forcing large-scale circulations in the high southern latitudes. *J. Atmos. Sci.,* **51,** 3566–3579.

Schwerdtfeger, W., 1960: The seasonal variation of the strength of the southern circumpolar vortex. *Mon. Wea. Rev.,* **88,** 203–208.

——, 1967: Annual and semi-annual changes of atmospheric mass over Antarctica. *J. Geophys. Res.,* **72,** 3543–3547.

——, 1984: *Weather and Climate of the Antarctic.* Elsevier, 261 pp.

——, and F. Prohaska, 1956: The semi-annual pressure oscillation, its cause and effects. *J. Meteor.,* **13,** 217–218.

Tzeng, R., D. H. Bromwich, and T. R. Parish, 1993: Present-day Antarctic climatology of the NCAR Community Climate Model Version 1. *J. Climate,* **6,** 205–226.

van Loon, H., 1967: The half-yearly oscillations in middle and high southern latitudes and the coreless winter. *J. Atmos. Sci.,* **24,** 472–486.

——, 1972: Pressure in the Southern Hemisphere. *Meteorology of the Southern Hemisphere, Meteor. Monogr.,* No. 35, Amer. Meteor. Soc., 59–86.

——, and J. C. Rogers, 1984: Interannual variations in the half-yearly cycle of pressure gradients and zonal wind at sea level on the Southern Hemisphere. *Tellus,* **36A,** 76–86.